Nano Res. 2010, 3(10): 714–721
DOI 10.1007/s12274-010-0035-3
Research Article

ISSN 1998-0124
CN 11-5974/O4

Towards Flexible All-Carbon Electronics: Flexible Organic Field-Effect Transistors and Inverter Circuits Using Solution-Processed All-Graphene Source/Drain/Gate Electrodes

Yongsheng Chen[1] (✉), Yanfei Xu[1], Kai Zhao[2], Xiangjian Wan[1], Jiachun Deng[2], and Weibo Yan[1]

[1] Key Laboratory of Functional Polymer Materials and Center for Nanoscale Science & Technology, Institute of Polymer Chemistry, College of Chemistry, Nankai University, Tianjin 300071, China

[2] Key Laboratory of Display Materials and Photoelectric Devices, Institute of Material Physics, Tianjin University of Technology, Tianjin 300384, China

Received: 4 August 2010 / Revised: 20 August 2010 / Accepted: 22 August 2010

ABSTRACT

Flexible organic field-effect transistors (OFETs) using solution-processable functionalized graphene for all the electrodes (source, drain, and gate) have been fabricated for the first time. These OFETs show performance comparable to corresponding devices using Au electrodes as the source/drain electrodes on SiO_2/Si substrates with Si as the gate electrode. Also, these devices demonstrate excellent flexibility without performance degradation over severe bending cycles. Furthermore, inverter circuits have been designed and fabricated using these all-graphene-electrode OFETs. Our results demonstrate that the long-sought dream for all-carbon and flexible electronics is now much closer to reality.

KEYWORDS

Solution processing, flexibility, all-graphene-electrode OFETs, inverter circuits

1. Introduction

Organic field-effect transistors (OFETs) are envisioned as the essential building blocks for state-of-the-art and next-generation electronics including displays, sensors, e-paper, and radiofrequency identification tags [1–5]. OFETs allow large-area flexible electronic devices to be fabricated at low cost [6–8], but to fully exploit these advantages in practical applications, solution fabrication processes are strongly desired [8–12]. Currently, metals like gold (Au) are widely used for the source/drain (S/D) electrodes in the fabrication of OFETs on SiO_2/Si substrates with Si as the gate (G) electrode, although large contact resistance generally exists between organic semiconductors and metal electrodes [13]. Moreover, utilization of these metal electrodes makes it rather difficult to have fully flexible and solution-processed devices and electronics. Thus, electrode materials with high carrier injection efficiency, excellent interface compatibility with organic semiconductors and, epecially, easy solution processability and suitability for use in flexible electronics are in high demand.

Graphene, a unique two-dimensional monolayer of sp^2-bonded carbon atoms, has been studied for many device applications owing to its many remarkable electronic [14–19] and mechanical [20, 21] properties. In particular, its high carrier mobility, appropriate

Address correspondence to yschen99@nankai.edu.cn

work function, good optical transparency, and high chemical stability make it a very promising electrode and active material in all-carbon electronic devices and electronics [22–28]. Recently, several different OFETs have been fabricated using graphene to replace the conventional Au as S/D electrodes on SiO_2/Si substrates [13, 29–32]. Also, significant progress has been made in the use of solution-processed organic materials as the active layer in these devices [33, 34]. To date, there have been four major approaches to prepare graphene materials, namely epitaxial growth [35], chemical vapor deposition [36], mechanical peeling [37] and chemical exfoliation of graphite based on the early Hummers' method [38]. Of these methods, the chemical exfoliation method has advantages for large-scale production and affords graphene with good solution processability, which makes it an excellent practical choice as the electrode material in solution-processed and flexible electronic applications.

In this work, all-graphene-electrode (S/D/G electrodes) OFETs and inverter circuits have been fabricated using solution-processable functionalized graphene (SPFGraphene) as illustrated in Fig. 1, and shown to possess good electronic performance and mechanical flexibility. Proof-of-concept flexible OFETs with all-graphene-electrodes showed a mobility of 0.02 $cm^2/(V·s)$ and on/off ratio of approximately 10^6, when a vapor-deposited pentacene film was used as the organic semiconductor layer. Furthermore, these devices show excellent mechanical flexibility, without any degradation in performance even when bent with a radial angle of ~30°. A basic building block for integrated circuits (ICs), an inverter circuit, has also been designed and fabricated using these OFETs.

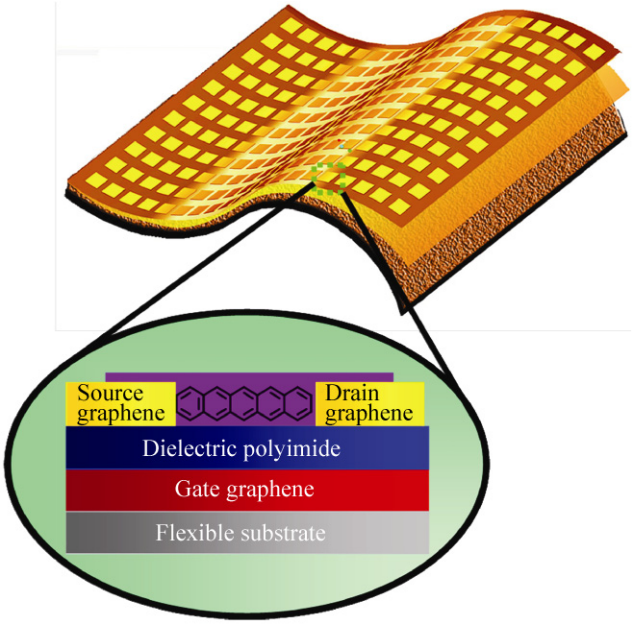

Figure 1 A schematic illustration of the structure of flexible bottom-contact OFETs based on a pentacene film. Graphene was used for all S/D/G electrodes, and polyimide was used as the dielectric layer. In the device fabrication, the G electrode (graphene), dielectric layer (polyimide), and S/D electrodes (graphene) were all fabricated by solution processes on a flexible polyimide substrate

2. Experimental

Patterned graphene electrodes and OFETs were fabricated as outlined in Fig. 2 (see the Electronic Supplementary Material (ESM) for a detailed description). A dispersion of SPFGraphene was prepared from natural graphite by a modified Hummers' method [39]. Typically, 10 mg/mL of SPFGraphene dispersion was sonicated for 3 h and subsequently spin coated at 500 r/m for 6 s and then at 3000 r/m for 10 s on cleaned polyimide substrates. After spin-coated deposition, the insulating SPFGraphene films were reduced through exposure to hydrazine vapor and then annealed in an inert atmosphere at 400 °C for 3 h with a heating rate of 5 °C/min to render the graphene film electrically conductive (a film with thickness of 40 nm had a conductivity of 7 S/cm). The above graphene film, as the G electrode, was then covered with a polymer dielectric (~10 μm) layer, prepared by spin-coating a solution of polyimide precursor (polyamic acid solution in *N*-methylpyrolidone (NMP) and dimethylacetamide (DMAc), 15%–16% *w*/*w*, viscosity, 14 000–15 000 mPa·s). To ensure that the polyimide precursors transformed thermally to polyimide coating films, and that all the solvent was removed from the polyimide film, the coated substrate was pre-baked at 80 °C for 1 h, 120 °C for 1 h, and finally cured at 250 °C for 2 h. The resulting dielectric layer had a capacitance (Ci) of 0.3 nF/cm. An atomic force microscopy (AFM) image of the polyimide dielectric surface is shown in Fig. S-1 (in the ESM). Finally, 5 mg/mL of SPFGraphene dispersion was drop-cast on the dielectric layer through a shadow mask to form the S/D pre-electrodes [29] (see the ESM for details). These S/D pre-electrodes were reduced

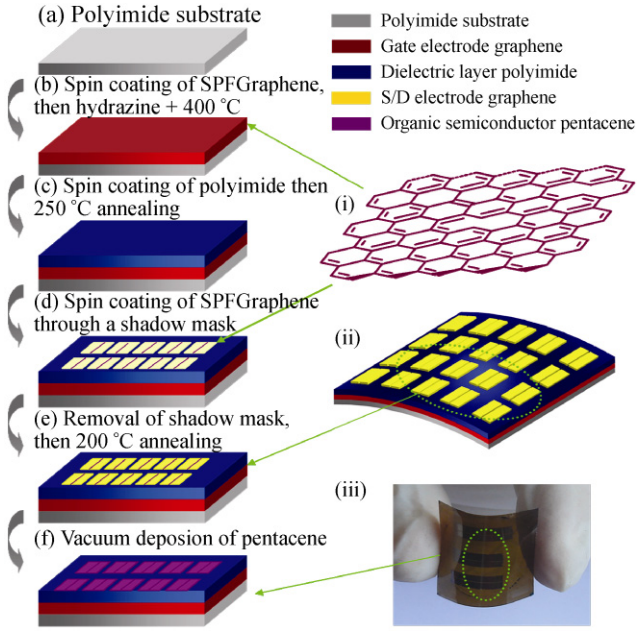

Figure 2 A schematic representation of the fabrication of OFETs with graphene S/D/G electrodes. (a)–(f) Schematic illustration of the fabrication of pentacene OFET devices. (i) Structure of graphene; (ii) a schematic representation of the unfinished OFET before adding the pentacene layer, showing its good flexibility; (iii) the finished pentacene OFET on a flexible polyimide substrate when bent under force. It should be noted that the electrode thickness of the G and S/D electrodes using this solution-processable functionalized graphene should in principle be controllable, which should facilitate future device optimization

by annealing under an inert atmosphere at 200 °C for 30 min with a heating rate of 5 °C/min to render the graphene films electrically conductive (the films had a thickness of ~50 nm and conductivity of ~0.6 S/cm). For bottom contact OFET device fabrication, pentacene was vacuum-deposited onto substrates at a rate of 0.2–0.3 Å/s (room temperature, base vacuum of 5×10^{-4} Pa, thickness ~800 nm). An SEM image of the polycrystalline pentacene layer on the channel is shown in Fig. S-2 (in the ESM).

3. Results and discussion

The S/D graphene electrode pattern is outlined in Fig. 3(a) and an optical microscope image is shown in Fig. 3(b). The size of the graphene electrodes is controlled by the mask containing a channel length (L) of ~100 μm and width (W) of ~3 cm. The sharp and regular contact edges can be clearly seen from the AFM image in Fig. 3(c). The height profile (Fig. 3(d)) of the S/D electrodes in Fig. 3(c) indicates that the S/D electrode is ~50 nm thick.

Typical output and transfer characteristics of the all-graphene-electrode OFETs are illustrated in Figs. 4(a) and 4(b), respectively. The inset in Fig. 4(a) is the simplified equivalent circuit diagram for the all-graphene-electrode OFETs. Note in our FET testing, the gate is connected to the negative electrode and the source is connected to the positive electrode, so the value of V_{SG} (= $V_S - V_G$) is positive. These OFETs yield an average hole mobility of ~0.02 $cm^2/(V \cdot s)$, an on/off ratio of ~10^6, and a threshold voltage (V_T) of ~38 V over twenty devices. The gate leakage current is ~10 nA at gate biases (V_{SG}) of ~100 V. As is evident from the output curves illustrated in Fig. 4(a), there is a clear linear S/D current (I_{SD})–voltage relationship in the low S/D voltage (V_{SD}) region. This indicates the presence of an ideal ohmic contact between the S/D graphene electrodes and the pentacene layer [30]. This optimized contact resistance has been theoretically predicted for carbon-based materials [40], and previously observed for OFETs using graphene [30, 41] and carbon nanotubes [31, 40, 42] as the S/D electrodes. Compared with the OFET devices based on carbon

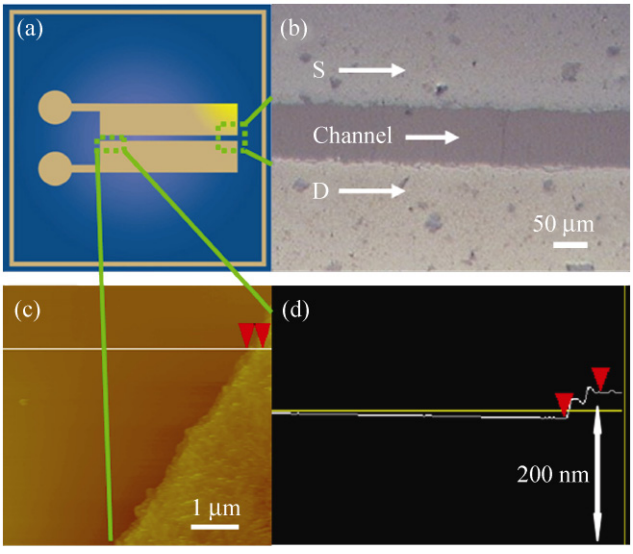

Figure 3 (a) A representation of the S/D graphene electrode pattern. (b) An optical microscopy image of the patterned graphene electrodes that serve as the S/D electrodes with L of ~100 μm. (c) An AFM image of the edge of the patterned S/D graphene electrodes. (d) The AFM height profile along the horizontal line in (c)

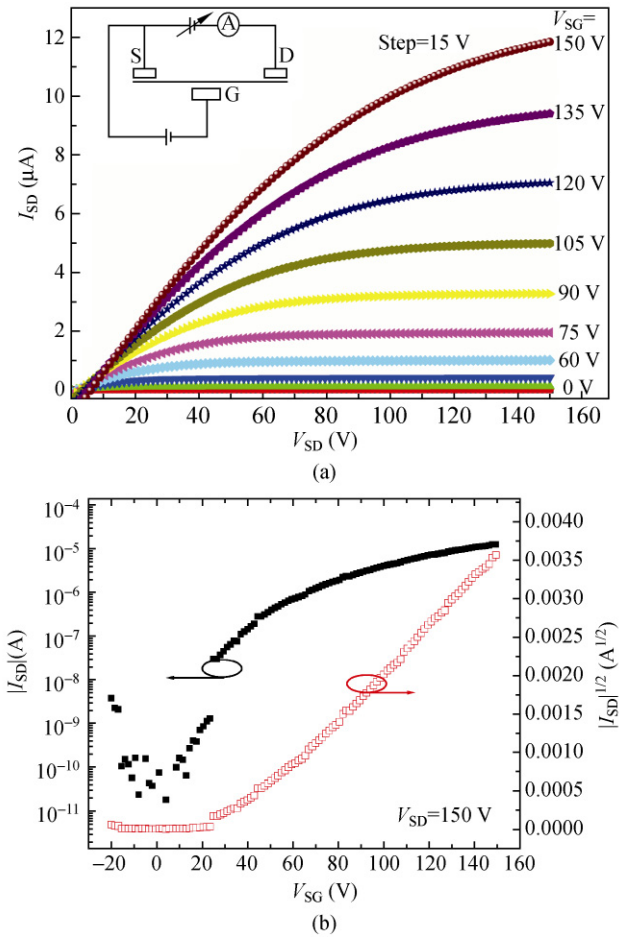

Figure 4 (a) Typical output characteristics for various values of V_{SG}. Inset: Simplified equivalent circuit diagram for the all-graphene-electrode OFETs. (b) Transfer characteristics at a constant V_{SD} of 150 V of all-graphene-electrode pentacene OFETs, with channel L of ~100 μm, W of ~3 cm, giving a hole mobility of 0.02 $cm^2/(V·s)$, an on/off ratio of approximately ~10^6, and V_T of ~38 V. Note in our FET tests, the gate is connected to the negative electrode and the source is connected to the positive electrode, so the value of V_{SG} (= V_S – V_G) is positive

nanotubes [42], we believe that the truly solution processing ability and high purity of graphene give it huge advantages over carbon nanotubes, particularly when flexible, large area and transparent devices are required.

Since the important goal in this work was to replace all conventional S/D (Au) electrodes and G (Si) electrodes simultaneously, we fabricated similar conventional pentacence OFETs with Au as the S/D electrodes on SiO_2/Si substrates as a comparison (see the ESM for details). The typical output and transfer characteristic curves for the devices are shown in Fig. S-3 (in the ESM). An average hole mobility of ~0.014 $cm^2/(V·s)$ with on/off ratio of ~10^6 and V_T of ~–20 V was obtained over twenty devices. The all-graphene-electrode OFETs showed good performance, comparable to the OFETs using Au as S/D electrodes on SiO_2/Si substrates, even under our unoptimized conditions. Also, the all-graphene-electrode OFETs show comparable performance to pentacene OFETs with similar structure using polyimide as the dielectric layer and Au as the material for all the electrodes [43, 44]. This indicates that flexible all-graphene-electrode OFETs can indeed be fabricated using solution processing, and give comparable—or even better—performance than conventional metal electrode OFETs.

To test the device flexibility and its performance when bent, transistor characteristic measurements were taken before, during, and after bending the device vertical/parallel to the channel over a radial angle of ~30° (as shown in the inset in Fig. 5). As expected, the device performance is completely recovered after both severe vertical and parallel bending (Fig. 5).

An important goal beyond the fabrication of these flexible OFETs via solution processing is to apply these all-graphene-electrode flexible OFETs in real IC applications. Therefore, using these flexible OFETs we have fabricated one of the most important building blocks for ICs—an inverter circuit—based a recently

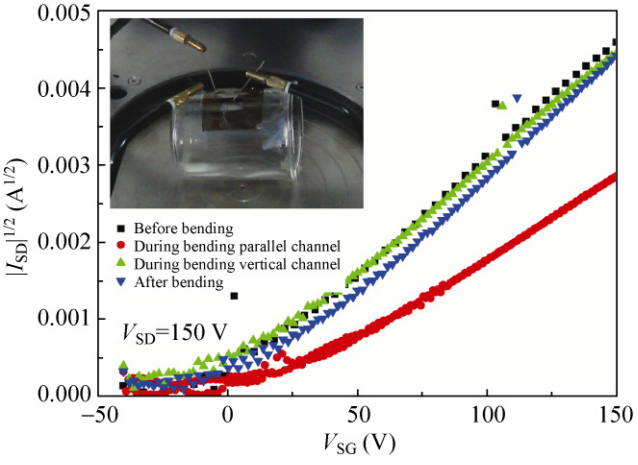

Figure 5 Transistor characteristics of a flexible all-graphene-electrode pentacene OFET, before bending, during bending at a radial angle of ~30° and after bending. The measurements were taken with an electrode bias V_{SD} of 150 V, channel L of ~100 μm, and W of ~3 cm. Inset: Photograph of a bent pentacene OFET with a radial angle of ~30° on a glass cup

reported design [45]. The circuits consisted of two pentacene OFETs mounted in series, including a load transistor (T_1, W_1/L_1 = 10 000 μm/270 μm) and a switching transistor (T_2, W_2/T_2 = 10 000 μm/70 μm), both of which were integrated within one polyimide substrate and had their respective G electrodes. The G electrode of T_1 (G_1) is connected to its drain (D_1) through the window on the polyimide dielectric layer. The input voltage (V_{in}) is applied to the G electrode of T_2 (G_2) and the output signal (V_{out}) is measured at the common node (Fig. 6).

The circuit was operated at various supply voltages (V_{DD}) from 100 to 200 V for V_{in} in the –50 to 200 V range (the inset in Fig. 7(a) shows the simplified equivalent circuit diagram for the inverter circuit). The voltage transfer and gain characteristics of the inverter circuits are shown in Fig. 7. The output voltage as a function of the input voltage of the inverter is shown in Fig. 7(a). The corresponding calculated gains (dV_{out}/dV_{in}) are shown in Fig. 7(b). The inverter operated at a maximum gain of 3 for V_{DD} = 200 V. Furthermore, the flexibility of the circuitry was also tested under tensile stress. Performance and characteristic measurements were taken before, during, and after bending the device vertical/parallel to the channel over a radial angle of ~30°. The changes to the transfer characteristics and the gain of the inverters induced by the bending are compared at V_{DD} = 200 V in Figs. 7(c) and 7(d). Although the performance of the inverter degrades under a tensile stress, the inverter transfer performance is recovered after each bending cycle.

It is important to note that although the all-graphene-electrode OFETs and inverter circuits show good

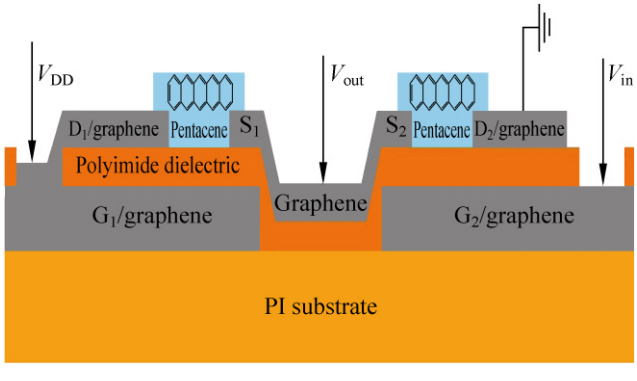

Figure 6 A schematic illustration of the structure of a flexible inverter circuit based on two all-graphene-electrode pentacene OFETs

performance, further efforts to improve their overall device performance including better mobility and lower operating voltage are still needed. A partial reason for expecting such improvements to be feasible lies in our current solution process. First, the work function of perfect graphene is believed to be ~4.6 eV [23], which should enable good ohmic hole injection into most organic semiconductors [13]. But, obviously, the work function should be optimized for each individual organic semiconductor material (pentacene in this case), and it is highly probable that this could be achieved by tailoring the defect (type and density) and edge shape of graphene [30, 46]. Second, the performance of our OFETs depends strongly on the Ci and thickness of the dielectric layer and the conductivity of the graphene electrode. Due to the solution process and the moderate temperature used to anneal the SPFGraphene layer, the conductivity of the graphene electrode is rather low compared with the values achieved with the higher annealing temperatures used for most reported graphene electrodes/films [22, 30]. Another issue in our case is that the polyimide dielectric layer we used has a relatively small Ci and high thickness. This results in a significant decrease in the device mobility [11, 47]. Furthermore, due to the limits of our fabrication facility, in order to have a complete solution process for all three electrodes, we could only reduce the channel length down to 70 μm using a drop cast technique; if the channel length could be made even smaller or other fabrication methods were used, the performance should be even better. Therefore, it is highly likely that with optimized graphene electrodes and dielectric layer, the performance of these all-graphene-electrode OFETs could be improved significantly [47, 48].

Most importantly, we want to point out that we used pentacene to demonstrate our proof-of-concept for all-graphene-electrodes OFETs and inverter circuits, as pentacene is believed to be one of the best OFET materials. Other organic semiconductor materials including graphene itself (in fact, pentacene can be considered as one of the smallest examples of graphene [2, 3]) and solution-processable polymer semiconductors (such as poly(3-hexylthiophene (P_3HT)) can also be used as the OFET active layer. Thus, if graphene materials with different electronic properties

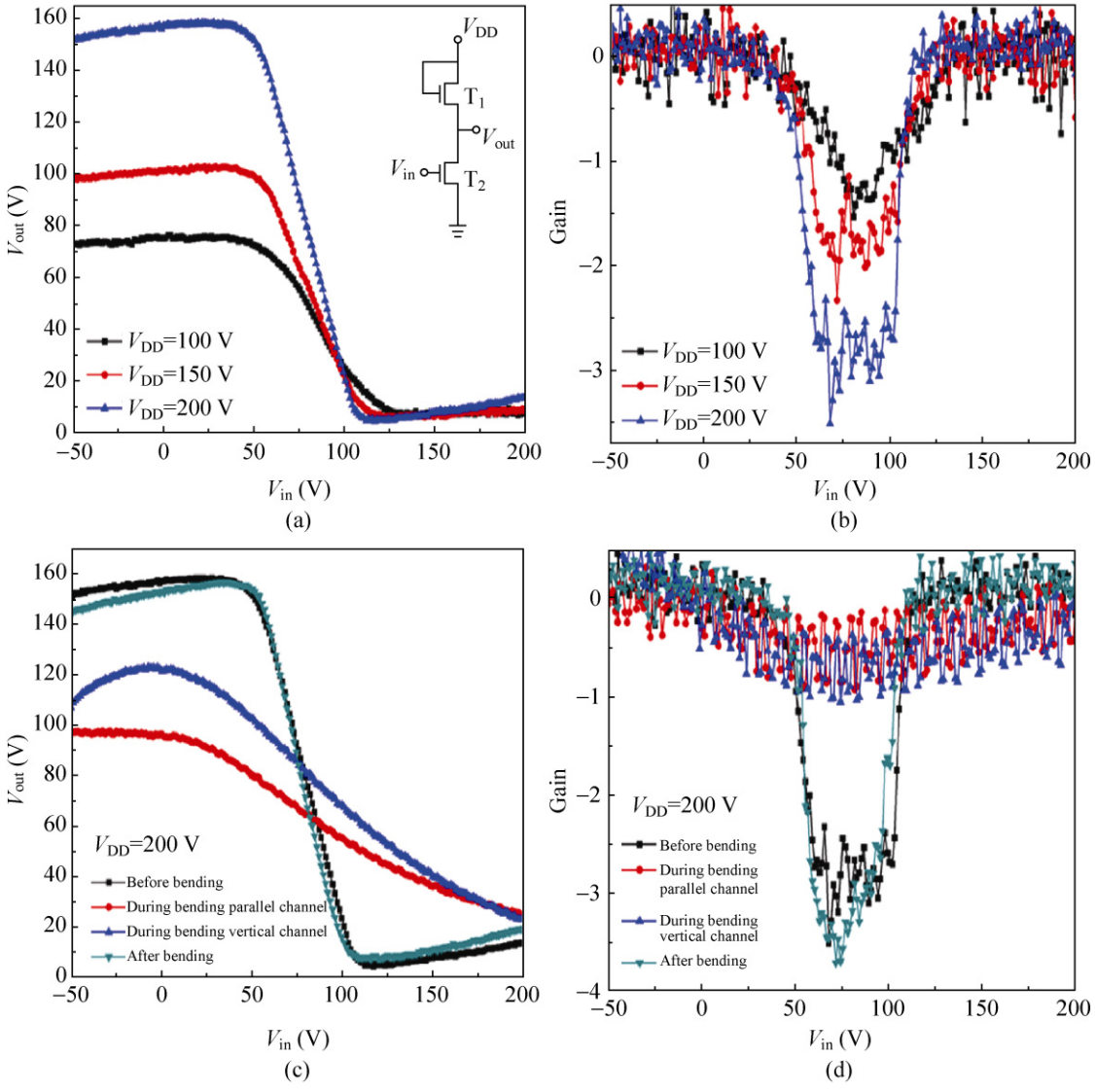

Figure 7 (a) Voltage transfer characteristics of the inverter fabricated using two flexible all-graphene-electrode pentacene OFETs at various V_{DD} = 100 V, 150 V, and 200 V. Inset: Simplified equivalent circuit diagram for the inverter circuit. (b) Calculated gain corresponding to the voltage transfer characteristics. The inverter operates at a maximum gain of 3 for V_{DD} = 200 V. (c) Inverter circuit characteristics before the bending, during bending at a radial angle of ~30° and after the bending. Voltage transfer characteristics at various V_{DD} = 200 V. (d) Calculated gain corresponding to the voltage transfer characteristics in (c)

(band structure/doping) are used, it should be only a matter of time before fully flexible all-carbon OFETs and electronics—where all the electrodes, connecting wires, as well as the active material are all graphene—can be fabricated using a complete solution process [22].

4. Conclusions

We have demonstrated the first solution-processed, all-graphene-electrode OFETs and inverter circuits with good electronic performance. Furthermore, when fabricated on flexible plastic substrates, the devices show great mechanical flexibility without performance degradation. Although further optimization is required to improve the performance of these OFETs, our work has demonstrated the exciting perspectives for fabricating flexible all-carbon and all solution-processed OFETs and other electronic devices with comparable performance to Si-based devices. Based on these results, we believe that the realization of

the long-sought goal of all-carbon flexible organic electro- nics using solution processing is much closer than previously thought.

Acknowledgements

The authors acknowledge financial support from the National Natural Science Foundation of china (NSFC) (Nos. 50933003, 20774047), the Ministry of Science and Technology of the People's Repulic of China (MOST) (No. 2009AA032304), and Natural Science Foundation (NSF) of Tianjin City (No. 08JCZDJC25300).

Electronic Supplementary Material: Supplementary material (experimental details, AFM image of the polyimide dielectric surface, SEM image of the polycrystalline pentacene layer on the channel and typical output and transfer characteristic curves of the OFETs with Au as S/D electrodes on an SiO_2/Si substrate) is available in the online version of this article at http://dx.doi.org/10.1007/s12274-010-0035-3 and is accessible free of charge.

References

[1] Braga, D.; Horowitz, G. High-performance organic field-effect transistors. *Adv. Mater.* **2009**, *21*, 1473–1486.

[2] Burghard, M.; Klauk, H.; Kern, K. Carbon-based field-effect transistors for nanoelectronics. *Adv. Mater.* **2009**, *21*, 2586–2600.

[3] Avouris, P.; Chen, Z. H.; Perebeinos, V. Carbon-based electronics. *Nat. Nanotechnol.* **2007**, *2*, 605–615.

[4] Sekitani, T.; Yokota, T.; Zschieschang, U.; Klauk, H.; Bauer, S.; Takeuchi, K.; Takamiya, M.; Sakurai, T.; Someya, T. Organic nonvolatile memory transistors for flexible sensor arrays. *Science* **2009**, *326*, 1516–1519.

[5] Kushmerick, J. Molecular transistors scrutinized. *Nature* **2009**, *462*, 994–995.

[6] Sun, Y. M.; Liu, Y. Q.; Zhu, D. B. Advances in organic field-effect transistors. *J. Mater. Chem.* **2005**, *15*, 53–65.

[7] Muccini, M. A bright future for organic field-effect transistors. *Nat. Mater.* **2006**, *5*, 605–613.

[8] Allard, S.; Forster, M.; Souharce, B.; Thiem, H.; Scherf, U. Organic semiconductors for solution-processable field-effect transistors (OFETs). *Angew. Chem., Int. Ed.* **2008**, *47*, 4070–4098.

[9] Baca, A. J.; Ahn, J. H.; Sun, Y. G.; Meitl, M. A.; Menard, E.; Kim, H. S.; Choi, W. M.; Kim, D. H.; Huang, Y.; Rogers, J. A. Semiconductor wires and ribbons for high-performance flexible electronics. *Angew. Chem. Int. Ed.* **2008**, *47*, 5524–5542.

[10] Liu, P.; Wu, Y. L.; Li, Y. N.; Ong, B. S.; Zhu, S. P. Enabling gate dielectric design for all solution-processed, high-performance, flexible organic thin-film transistors. *J. Am. Chem. Soc.* **2006**, *128*, 4554–4555.

[11] Ortiz, R. P.; Facchetti, A.; Marks, T. J. High-κ organic, inorganic, and hybrid dielectrics for low-voltage organic field-effect transistors. *Chem. Rev.* **2010**, *110*, 205–239.

[12] Facchetti, A.; Yoon, M. H.; Marks, T. J. Gate dielectrics for organic field-effect transistors: New opportunities for organic electronics. *Adv. Mater.* **2005**, *17*, 1705–1725.

[13] Di, C. A.; Wei, D. C.; Yu, G.; Liu, Y. Q.; Guo, Y. L.; Zhu, D. B. Patterned graphene as source/drain electrodes for bottom-contact organic field-effect transistors. *Adv. Mater.* **2008**, *20*, 3289–3293.

[14] Geim, A. K. Graphene: Status and prospects. *Science* **2009**, *324*, 1530–1534.

[15] Castro Neto, A. H.; Guinea, F.; Peres, N. M. R.; Novoselov, K. S.; Geim, A. K. The electronic properties of graphene. *Rev. Mod. Phys.* **2009**, *81*, 109–162.

[16] Eda, G.; Fanchini, G.; Chhowalla, M. Large-area ultrathin films of reduced graphene oxide as a transparent and flexible electronic material. *Nat. Nanotechnol.* **2008**, *3*, 270–274.

[17] Liu, Z. F.; Liu, Q.; Huang, Y.; Ma, Y. F.; Yin, S. G.; Zhang, X. Y.; Sun, W.; Chen, Y. S. Organic photovoltaic devices based on a novel acceptor material: Graphene. *Adv. Mater.* **2008**, *20*, 3924–3930.

[18] Eda, G.; Chhowalla, M. Graphene-based composite thin films for electronics. *Nano Lett.* **2009**, *9*, 814–818.

[19] Li, X. S.; Cai, W. W.; An, J. H.; Kim, S.; Nah, J.; Yang, D. X.; Piner, R.; Velamakanni, A.; Jung, I.; Tutuc, E., et al. Large-area synthesis of high-quality and uniform graphene films on copper foils. *Science* **2009**, *324*, 1312–1314.

[20] Lee, C.; Wei, X. D.; Kysar, J. W.; Hone, J. Measurement of the elastic properties and intrinsic strength of monolayer graphene. *Science* **2008**, *321*, 385–388.

[21] Dikin, D. A.; Stankovich, S.; Zimney, E. J.; Piner, R. D.; Dommett, G. H. B.; Evmenenko, G.; Nguyen, S. T.; Ruoff, R. S. Preparation and characterization of graphene oxide paper. *Nature* **2007**, *448*, 457–460.

[22] Becerril, H. A.; Mao, J.; Liu, Z.; Stoltenberg, R. M.; Bao, Z.; Chen, Y. Evaluation of solution-processed reduced graphene oxide films as transparent conductors. *ACS Nano* **2008**, *2*, 463–470.

[23] Yu, Y. J.; Zhao, Y.; Ryu, S.; Brus, L. E.; Kim, K. S.; Kim, P. Tuning the graphene work function by electric field effect. *Nano Lett.* **2009**, *9*, 3430–3434.

[24] Li, X. S.; Zhu, Y. W.; Cai, W. W.; Borysiak, M.; Han, B. Y.; Chen, D.; Piner, R. D.; Colombo, L.; Ruoff, R. S. Transfer of large-area graphene films for high-performance transparent conductive electrodes. *Nano Lett.* **2009**, *9*, 4359–4363.

[25] Kim, K. S.; Zhao, Y.; Jang, H.; Lee, S. Y.; Kim, J. M.; Kim, K. S.; Ahn, J. H.; Kim, P.; Choi, J. Y.; Hong, B. H. Large-scale pattern growth of graphene films for stretchable transparent electrodes. *Nature* **2009**, *457*, 706–710.

[26] Wang, Y.; Chen, X. H.; Zhong, Y. L.; Zhu, F. R.; Loh, K. P. Large area, continuous, few-layered graphene as anodes in organic photovoltaic devices. *Appl. Phys. Lett.* **2009**, *95*, 063302.

[27] Katsnelson, M. I. Graphene: Carbon in two dimensions. *Mater. Today* **2007**, *10*, 20–27.

[28] Wu, J. B.; Agrawal, M.; Becerril, H. A.; Bao, Z. N.; Liu, Z. F.; Chen, Y. S.; Peumans, P. Organic light-emitting diodes on solution-processed graphene transparent electrodes. *ACS Nano* **2010**, *4*, 43–48.

[29] Wang, S. A.; Ang, P. K.; Wang, Z. Q.; Tang, A. L. L.; Thong, J. T. L.; Loh, K. P. High mobility, printable, and solution-processed graphene electronics. *Nano Lett.* **2010**, *10*, 92–98.

[30] Pang, S. P.; Tsao, H. N.; Feng, X. L.; Mullen, K. Patterned graphene electrodes from solution-processed graphite oxide films for organic field-effect transistors. *Adv. Mater.* **2009**, *21*, 3488–3491.

[31] Cao, Y.; Steigerwald, M. L.; Nuckolls, C.; Guo, X. F. Current trends in shrinking the channel length of organic transistors down to the nanoscale. *Adv. Mater.* **2010**, *22*, 20–32.

[32] Lee, C. G.; Park, S.; Ruoff, R. S.; Dodabalapur, A. Integration of reduced graphene oxide into organic field-effect transistors as conducting electrodes and as a metal modification layer. *Appl. Phys. Lett.* **2009**, *95* 023304.

[33] Li, X. L.; Wang, X. R.; Zhang, L.; Lee, S. W.; Dai, H. J. Chemically derived, ultrasmooth graphene nanoribbon semiconductors. *Science* **2008**, *319*, 1229–1232.

[34] Jin, M.; Jeong, H. K.; Yu, W. J.; Bae, D. J.; Kang, B. R.; Lee, Y. H. Graphene oxide thin film field effect transistors without reduction. *J. Phys. D: Appl. Phys.* **2009**, *42*, 135109.

[35] Berger, C.; Song, Z. M.; Li, X. B.; Wu, X. S.; Brown, N.; Naud, C.; Mayou, D.; Li, T. B.; Hass, J.; Marchenkov, A. N., et al. Electronic confinement and coherence in patterned epitaxial graphene. *Science* **2006**, *312*, 1191–1196.

[36] Reina, A.; Jia, X. T.; Ho, J.; Nezich, D.; Son, H. B.; Bulovic, V.; Dresselhaus, M. S.; Kong, J. Large area, few-layer graphene films on arbitrary substrates by chemical vapor deposition. *Nano Lett.* **2009**, *9*, 30–35.

[37] Novoselov, K. S.; Geim, A. K.; Morozov, S. V.; Jiang, D.; Zhang, Y.; Dubonos, S. V.; Grigorieva, I. V.; Firsov, A. A. Electric field effect in atomically thin carbon films. *Science* **2004**, *306*, 666–669.

[38] Hummers, W. S.; Offeman, R. E. Preparation of graphitic oxide. *J. Am. Chem. Soc.* **1958**, *80*, 1339.

[39] Xu, Y. F.; Liu, Z. B.; Zhang, X. L.; Wang, Y.; Tian, J. G.; Huang, Y.; Ma, Y. F.; Zhang, X. Y.; Chen, Y. S. A graphene hybrid material covalently functionalized with porphyrin: Synthesis and optical limiting property. *Adv. Mater.* **2009**, *21*, 1275–1279.

[40] Qian, Z. K.; Hou, S. M.; Ning, J.; Li, R.; Shen, Z. Y.; Zhao, X. Y.; Xue, Z. Q. First-principles calculation on the conductance of a single 1,4-diisocyanatobenzene molecule with single-walled carbon nanotubes as the electrodes. *J. Chem. Phys.* **2007**, *126*, 084705.

[41] Cao, Y.; Liu, S.; Shen, Q.; Yan, K.; Li, P. J.; Xu, J.; Yu, D. P.; Steigerwald, M. L.; Nuckolls, C.; Liu, Z. F., et al. High-performance photoresponsive organic nanotransistors with single-layer graphenes as two-dimensional electrodes. *Adv. Funct. Mater.* **2009**, *19*, 2743–2748.

[42] Cao, Q.; Rogers, J. A. Ultrathin films of single-walled carbon nanotubes for electronics and sensors: A review of fundamental and applied aspects. *Adv. Mater.* ***2009****, 21,* 29–53.

[43] Fukuda, K.; Sekitani, T.; Someya, T. Effects of annealing on electronic and structural characteristics of pentacene thin-film transistors on polyimide gate dielectrics. *Appl. Phys. Lett.* **2009**, *95*, 023302.

[44] Kato, Y.; Iba, S.; Teramoto, R.; Sekitani, T.; Someya, T.; Kawaguchi, H.; Sakurai, T. High mobility of pentacene field-effect transistors with polyimide gate dielectric layers. *Appl. Phys. Lett.* **2004**, *84*, 3789–3791.

[45] Graz, I. M.; Lacour, S. P. Flexible pentacene organic thin film transistor circuits fabricated directly onto elastic silicone membranes. *Appl. Phys. Lett.* **2009**, *95*, 243305.

[46] Ramprasad, R.; von Allmen, P.; Fonseca, L. R. C. Contributions to the work function: A density-functional study of adsorbates at graphene ribbon edges. *Phys. Rev. B* **1999**, *60*, 6023–6027.

[47] Veres, J.; Ogier, S.; Lloyd, G.; de Leeuw, D. Gate insulators in organic field-effect transistors. *Chem. Mater.* **2004**, *16*, 4543–4555.

[48] Di, C. A.; Liu, Y. Q.; Yu, G.; Zhu, D. B. Interface engineering: An effective approach toward high-performance organic field-effect transistors. *Acc. Chem. Res.* **2009**, *42*, 1573–1583.